Available online at www.sciencedirect.com

ScienceDirect

Procedia Materials Science 8 (2015) 73 – 81

Procedia Materials Science

www.elsevier.com/locate/procedia

International Congress of Science and Technology of Metallurgy and Materials, SAM - CONAMET 2013

Implementation of Different Techniques for Monitoring the Corrosion of Rebars Embedded in Concretes Made with Ordinary and Pozzolanic Cements

D. R. Vazquez[*a,b], Y. A. Villagrán Zaccardi[c,d], C. J. Zega[c,d], M. E. Sosa[c,d], G. S. Duffó[a,b,c]

[a]*Instituto Sabato, Universidad Nacional de General San Martín (UNSAM),San Martín (1650), Argentina.*
[b]*Comisión Nacional de Energía Atómica (CNEA), San Martín (1650), Argentina.*
[c]*Comisión Nacional de Investigaciones Científicas y Técnicas (CONICET), San Martín (1650), Argentina.*
[d]*Laboratoruio de Entrenamiento Multidisciplinario para la Investigación Tecnológica (LEMIT), La Plata (1900), Argentina.*

Abstract

For the development of an intermediate radioactive waste repository, two different types of reinforced concrete were analyzed in terms of durability: one made with ordinary portland cement and the other one made with pozzolanic cement. The values for compressive strength, sorptivity and air permeability demonstrate that the formulations are compatible with the required application. The corrosion rate of rebar up to about 300 days of monitoring and obtained with sensors is below the threshold value required for this type of facilities, except when temperatures are high. The value for the same parameter monitored by the galvanostatic pulse technique using superficial counter electrode and guard electrode is always lower than the threshold value. Additionally, when applying the galvanostatic pulse technique using embedded electrodes, this parameter is comparable to the guard electrode method only when the polarization resistance is calculated through non-linear fitting.

Selection and peer-review under responsibility of the scientific committee of SAM - CONAMET 2013

Keywords: radioactive waste, corrosion, reinforced concrete durability.

* Corresponding author. Tel.: +549-011-67727347.
E-mail address: dvazquez@cnea.gov.ar

Selection and peer-review under responsibility of the scientific committee of SAM - CONAMET 2013
doi:10.1016/j.mspro.2015.04.050

1. Introduction

The study of the corrosion in reinforced concrete of done by means of different parameters analysis, in addition to the corrosion potential and the corrosion rate. To mention some of them, the electrical resistivity of the concrete, the carbonation rate, environmental temperature, temperature and availability of oxygen inside of the material, etc. These parameters are usually monitored by embedded sensors, which have the advantage of being non-invasive for the structures as was reported by Martinez and Andrade (2009), and Duffó and Farina (2003). In addition, there are commercial instruments that implement different non-destructive techniques to measure different parameters separately, among these, the electrical resistivity of the concrete, the corrosion potential and the corrosion rate of the reinforcement, as described by Martinez and Andrade (2009). In this context, there are different methods to determine the corrosion rate and the difference lies in the way to measure and determinate the value of the polarization resistance (Rp). Once obtained Rp value, it is possible to calculate the corrosion current density with the Stern and Geary equation (1957), i=B/Rp, where the constant B was determined and reported by Andrade and Gonzalez (1978).

The two most commonly used techniques for the determination of Rp are the galvanostatic pulse and the linear polarization resistance (LPR) technics. The galvanostatic pulse technic is based on the application of a constant-current pulse, during a certain period of time, between the working electrode (WE) and the counter electrode (CE), registering the evolution of the WE potential respect to a reference electrode (RE). In a galvanostatic condition, the evolution of the potential can be modeled trough Randles circuit as follows: $E(t)=I * Rs+ I * Rp * (1-\exp(-t/C * Rp))$, Gonzalez and Cobo (2001). In this equation, I is the value of the applied current, Rs is the electrical resistance of the concrete between the WE and the ER, C is the capacitance of the double layer and Rp is the polarization resistance. The current values applied must be low enough and during a time short enough to make sure that the relationship between the current and potential is linear and so, it is valid the Stern-Geary equation. Gonzalez and Cobo (2001) showed that the relation between I and E is linear when the polarization is lower than 80 mV for active steel and 50 mV for passive steel reinforcements. In the case of a reinforcement that is corroded actively, the system reaches a steady state after a short period of application of the galvanostatic pulse (the value of the potential reaches a constant value). Otherwise, if the metal is passivated, the system does not reach the steady state in a short period of time and the potential reached is high enough to deviate from the linear relationship with the current, as was showed by Gonzalez and Cobo (2001). In this case Rp can be estimated through a non-linear adjustment of the potential evolution (i.e. with the Randles model response above mentioned). On the other hand, in field measurements there are uncertainties in the determination of Rp, mainly associated with the lack of uniformity of the current lines between the reinforcements and the counter electrode. To solve this problem a technique based on a guard electrode was developed. This guard electrode allows the current to flow uniformly between the reinforcement (WE) and the the CE in a confined and known area between them. This technique is also based on the application of a galvanostatic pulse and the RE, the CE and the guard electrode are placed on the surface of the concrete, at the same level of the reinforcement area that is desirable to measure.

This work analyze and compare two concretes elaborated with different formulations, with ordinary portland cement and pozzolanic portland cement, from the durability and ability to be employed in the construction of an intermediate radioactive waste repository. The physic-mechanical properties of compressive strength, sorptivity and air permeability were measured. On the other hand, a monitoring of the different parameters associated with the corrosion of the reinforcement was carried out using corrosion sensors embedded in the two types of concretes and making measurements directly on the embedded rebar. The measurements on the embedded rebar were taken by two methods. In one of them the galvanostatic pulse technique is implemented with a guard electrode through a commercial instrument (GECOR 6), whose CE and RE are superficial, while in the other case embedded RE and CE were used. The results obtained with both forms of implementation of the galvanostatic pulse technique allowed us to make a comparison between the two types of concrete corrosion behavior, as well as the two ways of implementing the galvanostatic pulse technic. At the same time, the analysis of the evolution of the different parameters over longer period would make it possible to evaluate the feasibility of the implementation of these types of concretes in the construction of an intermediate level radioactive waste repository.

2. Experimental

The measurements were performed on four prototypes of reinforced concrete, two of them with ordinary portland cement (CPN) and the others with pozzolanic portland cement (CPP), whose dimensions are 50x60x15 cm^3. Both types of cements comply with the requirements of IRAM 50000 (2000) standard. The Table 1 specifies the chemical compositions and physical properties of both types of cements, Table 2 shows the proportions of the different constituents used in the elaboration of the concretes and Table 3 specifies the properties in the fresh state of mixtures. The coarse aggregate used was granitic crushed stone of nominal maximum size of 19 mm and the fine aggregate was river siliceus sand; the properties of the aggregates are shown in Table 4. The dosages of the admixtures were defined to ensure low of mortar content compatible with the required consistency. This possibility was given by the use of high and intermediate-range water reducer, whose properties are presented in Table 5.

Table 1. Chemical compositions and physical properties of the used cements.

Chemical Composition		CPN	CPP
Ignition (%)		0.87	1.20
Insoluble Residue (%)		2.65	21.65
Sulfur Trioxide (SO_3) (%)		1.73	1.40
Magnesium Oxide (MgO) (%)		1.60	1.01
Silicon Dioxide (SiO_2) (%)		19.86	14.79
Ferric Oxide (Fe_2O_3) (%)		4.19	3.09
Aluminum Oxide (Al_2O_3) (%)		4.11	4.77
Calcium Oxide (CaO) (%)		63.82	50.32
Sodium Oxide (Na_2O) (%)		0.01	0.16
Potassium Oxide (K_2O) (%)		0.93	1.24
Chloride (Cl^-) (%)		0.03	0.03
Physical Properties			
Fineness	Blaine (m^2/kg)	288	281
	Mass retained in sieve 75μm	2.4	2.1
Compressive Strength (MPa)	2 days	20.4	18.9
	28 days	44.4	41.8
Density (g/cm^3)		3.13	2.95

Table 2. Proportions of constituents in concretes.

Materials	Concretes	
	CPN	CPP
Water	140	140
Cement	400	-
Fine Aggregate	920	895
Coarse Aggregate	980	980
Additive M	3.2	4.0
Additive D	6.0	8.0
Fresh State	CPN	CPP
Slump (mm)	185	200
Unitary weight (kg/m^3)	2442	2414
Entrained air (%)	3.5	4.3

Table 3. Properties in the fresh state of mixtures.

	CPN	CPP
Slump (mm)	185	200
Unitary weight (kg/m^3)	2442	2414
Entrained air (%)	3.5	4.3

Each prototype was reinforced with four bars and an electro-welded mesh Sima® with 150 mm grid, in both cases, the diameter of these frames is 10 mm and were manufactured by Acindar Company. The chemical composition of the steel rebar is the following: C, 0.41 %; Mn, 0.73 %; Cu, 0.27 %; Ni, 0.13 %; Si, 0.28 %; P, <0.01%; S, 0.02%; N, 0.008%; Fe, balance. The coating thickness of the mesh was of 50 mm with respect to one of the faces of 50x60 cm^2 and each bar was placed in the same way as the mesh but with respect to the analogue opposite face. Figure 1 (a) shows a view of the position of the bars, the mesh, the counter electrodes and the reference electrodes, that will be described later. The figures 1 (b) and (c) show a cross sectional view of the prototypes and in these figures the position of the bars and the mesh can be appreciated. The exposed length of the bars is of 200 mm, which was demarcated with epoxy paint. The bars, as well as the meshes have welded copper contacts, extending toward the outside to allow connections for the electrochemical measurements. Every welding was sealed with epoxy resin to avoid its deterioration. The prototypes were exposed to the external environment, on a building roof placed in Constituyentes Atomic Center, which is a research center related to nuclear energy

applications in Buenos Aires city. The CPN prototypes, as well as the CPP ones, were in perpendicular positions one to each other, simulating a corner between two walls of a radioactive waste container (figure 1 (d)).

For each type of concrete was also prepared cylindrical specimens of 10x20 cm^2 to determinate following properties of the hardened concrete: compression strength at the age of 28 and 90 days and sorptivity at the age of 28 days. These specimens were cured in a fog room (T: 23± 2 °C; HR > 95 %) until age of each test. The compressive strength was determined according to the IRAM 1534 (1985), 1546 (1992) and 1553 (1983) standards. The sorptivity and the sorption capacity were determined in samples of 10x5 cm^2 in diameter and height, according to the IRAM 1871 (2004) standard, obtained from the sawing of longer cylinders.

Tabla 4. Aggregate properties.

	Aggregates	
	Fine	Coarse
Fineness Modulus	2.30	6.71
Density s.d.s.	2.67	2.75
Water Absorption (%)	0.5	0.2

Tabla 5. Characteristic of the dosages.

Type	Density	Composition	Solid Content (%)
M	1.142	Modified Lignosulfonate	52.7
D	1.158	Naphtalene Sulfonate	49.3

After the standardized curing of the prototypes, the air permeability by the Torrent method was determined, SIA 262/1 Annex E (2003). This method uses a device that generates a vacuum in a chamber on the concrete surface. The permeability is determined from the vacuum loss rate in the chamber due to the air flow from the concrete. To ensure unidirectional air flow, the method limits the measurement to a volume of concrete defined by the suction of a second external and concentric auxiliary camber. The measurements were made two days after prototypes were removed from the fog room, and repeated 15 days later.

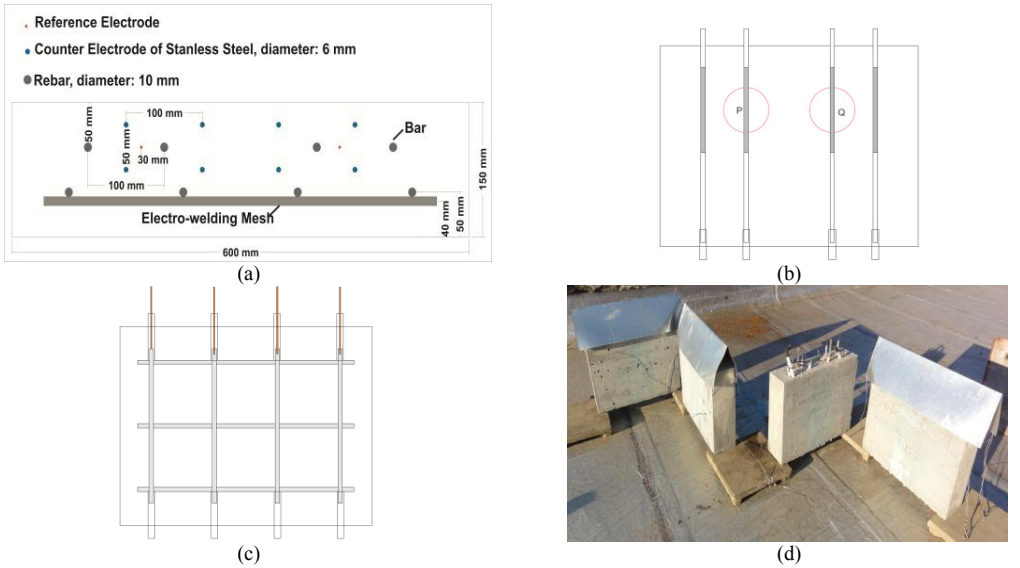

Figure 1. (a) View of the electrodes and rebar position. (b) and (c) Cross sectional view of the position of the rebar in the prototypes. (d) Prototypes exposed to the external environment.

Each prototype was instrumented with two embedded corrosion sensors, developed by Duffó and Farina (2003), which allow the simultaneous monitoring of the following parameters: corrosion potential, corrosion rate, electrical resistivity of the concrete, availability of oxygen and temperature inside the prototype. In each prototype one sensor was attached to a bars (figure 1 (b)), and the other to the mesh, named as S1 and S2 for CPN prototype and S3 and S4 for CPP prototype.

In addition, measurements have been carried out to monitor the electrochemical corrosion rate on two of the steel bars in locations named as P and Q, as showed in figure 1 (b). The measurements were made using the galvanostatic pulse technique in two different ways: one of them is performed with a guard electrode, which is able to confine the current flow in a defined exposed length of 10.5 cm between the WE (bar) and the CE (stainless steel). This current can be considered homogeneous due to the fact that the measurement is located in a small region, Martinez and Andrade (2009). This measurement was made using the commercial instrument GECOR 6, GEOCISA, which applies a galvanostatic pulse for a time of 60 seconds. The instrument measures the corrosion rate by calculating the Rp value through a non-linear fitting of the potential response to the galvanostatic pulse. Another characteristic of the instrument is that it employs a guard electrode, the CE and the RE on the concrete surface at the same level of the area of the rebar that is wanted to measure.

The other method implemented for measuring the corrosion rate is based on the application of a galvanostatic pulse by means of CE and a RE embedded. The CE is made with stainless steel bars with a diameter of 6 mm and the RE is a wire of titanium coated with titanium oxide doped with iridium and tantalum, characterized as RE by Duffó et al. (2009). In order to maximize the uniformity in the current between the CE and the bar (WE) during measurements, it was placed four CE bars around each bar, presenting an exposed area of 3.5 times the exposed area of the bar. The galvanostatic pulse length is 60 s and the instrument used for these measurements is a Gamry potentiostat-galvanostat, model Reference 600.

3. Results and discussion

Compressive strength and sorptivity of concrete are shown in Table 6. For the compressive strength, CIRSOC Regulation, 201 (2005) can be considered as reference, which establishes a minimal value of 45 MPa for concretes for conventional structures, pre-stressed and in highly aggressive chemical environment. The compressive strength values here obtained were 55.3 and 42.8 MPa at 28 days and 60.7 and 55.9 MPa at 90 days for CPN and CPP concretes, respectively. In addition it should be considered the low water/cement ratio of 0.35. Likewise, the values of sorptivity also confirm the potential durability of concretes designed, as they are much lower than the limit of 4 $g/m^2/s^{1/2}$. However, these sorptivity values should not be considered completely on a quantitative basis, as indicated by IRAM 1871 (2004) methodology, which shows some uncertainties regarding the evaluation of very low sorptivity concretes, as was showed by Villagrán Zaccardi et al. (2012).

Table 6. Compressive strength and sorptitvity of the concretes.

Concrete	Compressive strength (MPa)				Sorptivity ($g/m^2/s^{1/2}$)	Sorption capacity (g/m^2)
	28 days		90 days			
	Mean	s	Mean	s		
CPN	58.1	2.2	62.1	1.1	1.31	820
CPP	48.4	4.4	60.3	3.4	1.68	908

Table 7. Torrent air permeability (10^{-16} m^2).

Prototype	Age (days)	Surface near the mesh		Surface near rebars		Mean
CPN1	30	0.007	0.008	0.025	0.002	0.011
	45	0.026	0.023	0.029	0.013	0.023
CPN2	30	0.004	0.009	0.028	0.004	0.011
	45	0.015	0.026	0.051	0.020	0.028
CPP1	30	0.002	0.001	0.008	0.023	0.009
	45	0.013	0.009	0.014	0.013	0.012
CPP2	30	0.001	<0.001	<0.001	0.010	0.003
	45	0.008	0.017	0.007	0.018	0.013

The results of air permeability (Torrent) are presented in Table 7. It can be noticed an increase in the values of permeability between the ages of 30 and 45 days, in correspondence with the greater drying experienced by the concrete along time: the values increase from $0.011*10^{-16}$ m^2 to 0.023 and $0.028*10^{-16}$ m^2 for the CPN prototypes.

The respective increases for CPP prototypes were 0,009 and $0.003*10^{-16}$ m^2 to 0.012 and $0.013*10^{-16}$ m^2, respectively. For CPP prototypes these values are slightly lower than those with CPN, but the differences are very small to infere an statistically significant difference. On the other hand, the young age of the concretes is not sufficient for the pozzolanic action in the CPP prototypes, which produces a noticeable difference. It is expected that the difference between permeability due to the type of cement were significantly increased with the increasing age of the concretes. In all cases, the reported values correspond with concretes of very low air permeability.

The physic-mechanical properties of the concretes showed to be consistent with a slow degradation over a period of 300 years in an environment with a low aggressiveness, according to NEA/CSNI/ R (2002). However, this postulate requires the observation of the lack of patterns of cracking which have an important influence on transport properties.

Figures 2 through 6 show the results of the parameters measured by the sensors as a function of time. Figure 2 (a) and (b) shows the measured temperature values for the prototypes of CPN and CPP, respectively. The internal temperatures are presented together with the ambient temperature. It can be seen that in general, the temperature inside the material is greater than that in the outside, with the largest recorded difference of 15.8 °C (belonging to sensor named as S1 bar). These differences are always high when the day is sunny, due to the material exposed to solar radiation storage thermal energy, raising its temperature respect to temperature the air, unlike the cloudy days when the temperatures of the material and environment are similar.

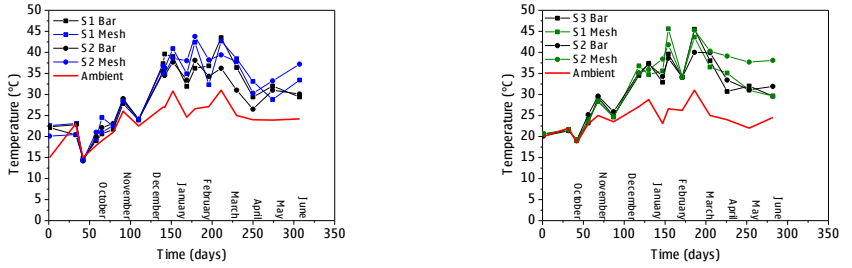

(a) (b)

Figure 2. Internal and ambient temperatures. (a) CPN. (b) CPP.

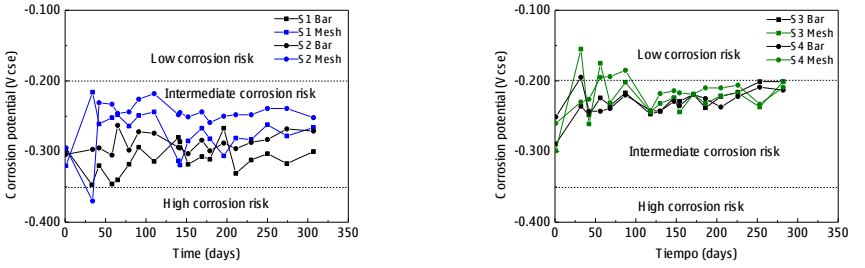

(a) (b)

Figure 3. Temporal evolution of the corrosion potential measured by the embbeded sensors. (a) CPN. (b) CPP.

The corrosion potential can be seen in Figure 3 (a) and (b) for CPN and CPP prototypes, respectively. It is distinguished that in both cases, their values belong to intermediate risk of corrosion range, according to the ASTM 876 (1991). It can be seen that in the CPP prototypes the values are in the limit between low and intermediate corrosion risk, unlike the CPN prototypes, whose values were scattered throughout the intermediate range.

In Figures 4 (a) and (b) it is possible to analyze the corrosion rate and its comparison with the temperature inside the CPN and CPP prototypes, respectively. It can be seen the impact of the temperature in the corrosion rate, so that the higher the temperature, the higher corrosion rate. It is noted that the corrosion is below the maximum limit value (indicated in dotted line) for intermediate radioactive waste repositories, according to Andrade et al. (1991), except in seasons of highest temperature when the recorded values exceed this limit.

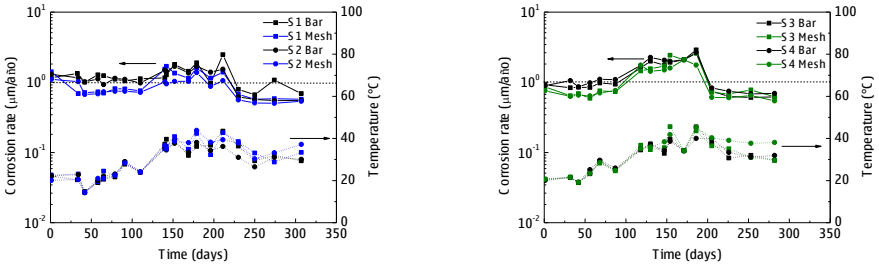

(a) (b)

Figure 4. Temporal evolution of the corrosión rate measured by the embbeded sensors. (a) CPN. (b) CPP.

In Figure 5 it is plotted the temporal evolution of the availability of oxygen expressed in µA/cm^2, together with the internal temperature. It can be seen that the oxygen flow has a similar behavior as the corrosion rate in relation with the temperature, being higher when the temperature is higher, reaching a maximum value of 100 µA/cm^2 for both type of concrete. It is worth to mention that oxygen is the main oxidizing agent for the rebar in contact with the pore alkaline liquid of the concrete; therefore the fact that the temperature increases the oxygen availability could also be associated with the increase in the corrosion rate in summer seasons.

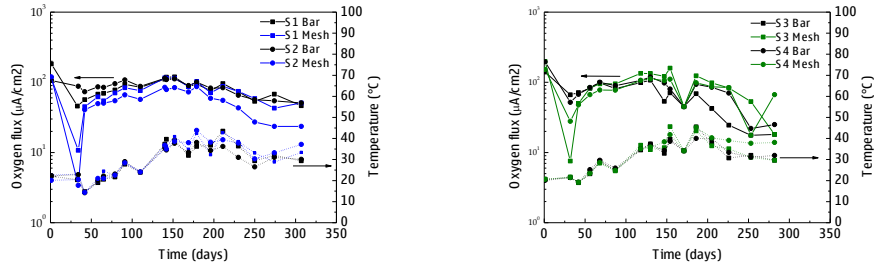

(a) (b)

Figure 5. Temporal evolution of the oxygen availability. (a) CPN. (b) CPP.

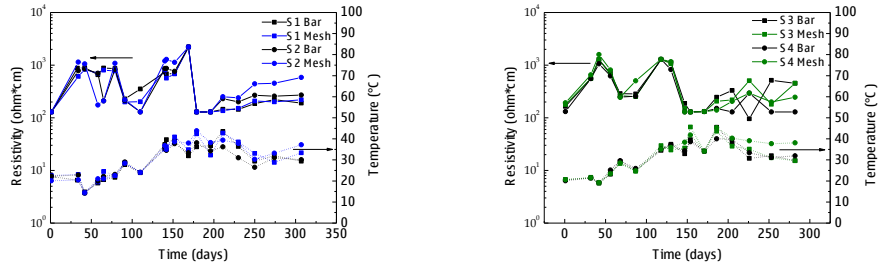

(a) (b)

Figure 6. Temporal evolution of the electric resistivity. (a) CPN. (b) CPP.

Figure 6 (a) and (b) plots correspond to the measurements of resistivity for both concretes and plotted together with the prototypes temperature values. It is expected that the higher temperature, the higher mobility of the ionic species dissolved in the pore liquid concrete and therefore it decreases the electrical resistivity, during the period of monitoring. However, this fact did not reflect such behavior. In both types of prototypes the values of this parameter are usually between 100 and 1000 Ω.cm. It would also be expected that this parameter will increase in time, due to the hydration processes of the material, which reduces the free water content in the pore.

Figure 7 (a) and (b) it is showed the evolution of the corrosion potential of the bars in each prototype, with respect to a copper electrode. In the case of the bars embedded in the CPN prototypes, the values are generally in the area of

low probability of active corrosion, although very close to the limit with intermediate risk and still do not show a growing trend. While in the CPP prototypes the values increase along time and after 100 days of monitoring the values changed from the intermediate corrosion risk to low corrosion risk.

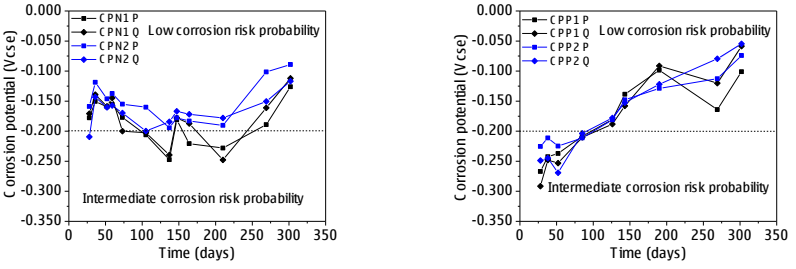

(a) (b)

Figure 7. Corrosion potential evolution of the embbeded bars, measured with the GECOR6 instrument. (a) CPN. (b) CPP.

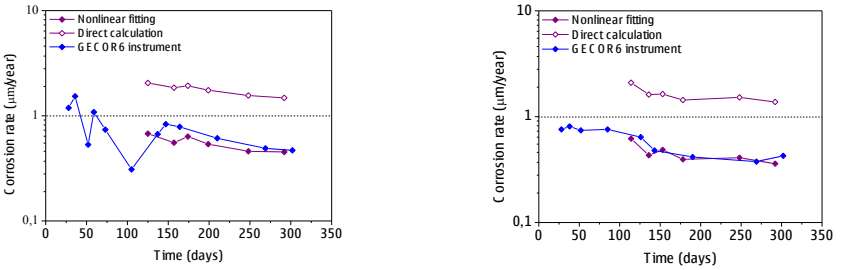

(a) (b)

Figure 8. (a) Corrosion rate evolution of the embbeded bars, measured with the GECOR6 instrument. (a) CPN. (b) CPP.

Figures 8 (a) and (b) show typical values of corrosion rates in the CPN and CPP prototypes, obtained by the GECOR 6 instrument and using embedded CE and RE. The measurements with embedded electrodes showed that when the galvanostatic pulse was applied, the potential did not reach the steady state up to 60 s, which is attributed to the presence of the passive layer on the surface of the reinforcement. Also, the values of the polarization at 60 s were aproximatly of 50 mV, the threshold polarization from wich the relation between the current and polarization aparts from linearity, according to Gonzalez and Cobo (2001). So, the value the corrosion rate was obtained by the Stern-Geary equation, calculating Rp by two different methods: one of them consists in subtracting the ohmic drop in the concrete to the polarization at the end of the measurement (60 s). In the second, the calculation is performed by a non-linear fitting, taking the Randles model and computing Rp as a fitting parameter. It can be seen that the values of the corrosion rate with embedded electrodes measurements and computing Rp with the non-linear fitting showed to be similar to the values obtained with GECOR 6 instrument. In both cases the values of corrosion rate are lower than the threshold value, in contrast with the values of corrosion rate obtained by Rp calculated from the subtraction. In this respect, it should be made the following considerations: the GECOR 6 instrument applies the galvanostatic pulse for 60 seconds and computes the Rp value from a six order polynomial fitting. On the other hand, the calculus of the corrosion rate using Rp from the subtraction is a conservative method, due to the polarizarion at the end of the measurement (60 s) is lower that the polarization in the steady state. In other words, the Rp values obtained from fittings are an estimation of this parameter in the steady state (long time of application of the signal) and consequently those values are higher and the corrosion rate is lower than the values calculated in a transient state (time of 60 s).

4. Conclusions

The physic-mechanical properties for both types of construction studied concretes demonstrate their aptitude for the application as intermediate level radioactive waste containers. Because the pozzolanic activity has a favorable influence in the long term, it should be expected that after a long term it will be able to appreciate physic-

mechanical differences between both kind of concretes and chose the most suitable for the required application. The corrosion potentials obtained with the sensors and for direct measurement on reinforcement bars demonstrate to be higher in the prototypes with pozzolanic portland cement than those in ordinary portland cement. The bars in the concrete with pozzolanic portland cement prototypes had have values low, but the general trend is favorable and to the present they correspond to the passive range.

The corrosion rate measured by the sensors is generally below the maximum limit recommended by the literature for this type of containers, except at high temperatures. Again, it is necessary to continue monitoring this parameter for longer time because it is expected a lower corrosion rate because of the constant drying evolution of the concrete, caused by hydration process.

The corrosion rate on the bars shows that the values obtained with the guard electrode and embedded electrodes techniques are similar, both being obtained by a calculation of Rp from a nonlinear fitting. Although these values are below the above mentioned limit, due to the short period of monitoring is not possible to obtain conclusions about the selection of a particular type of concrete for the required application.

References

I. Martinez and C. Andrade, Examples of reinforcement corrosion monitoring by embedded sensors in concrete structures. Cement & Concrete Composites, Vol. 32 (2009), p. 545-554.

G. S. Duffó and S. B. Farina, Development of an embeddable sensor to monitor the corrosion process of new and existing reinforced concrete structures, Construction and Building Materials, Vol. 23 (2003), p. 274-275.

M. Stern, A.L. Geary, Electrochemical Polarization: I. J. Electrochem. Soc., Vol. 104 (1957), p. 56-63.

Andrade and J. A. Gonzalez, Quantitative measurements of corrosion rate of reinforced steels embedded in concrete using polarization resistance measurements. Werkstoffe und Korrosion, Vol. 29, (1978), p. 515-519.

J. A. Gonzalez, A. Cobo, M. N. Gonzalez and S. Feliu, On-site determination of corrosion rate in reinforced concrete structures by use of galvanostatic pulses. Corrosion Science, Vol. 43 (2001), p. 611-625.

Cemento. Cemento para uso general. Composición, características, evaluación de la conformidad y condiciones de recepción. IRAM 50000 (2000), Buenos Aires, 31p.

IRAM 1534 (1985), Hormigón de Cemento Pórtland. Preparación y curado de probetas para ensayos en laboratorio. IRAM, Buenos Aires, 19p.

IRAM 1546 (1992), Hormigón de Cemento Pórtland. Método de ensayo de compresión. IRAM, Buenos Aires, 7p.

IRAM 1553 (1983), Hormigón de Cemento Pórtland. Preparación de probetas cilíndricas y testigos cilíndricos, para ensayo de compresión. IRAM, Buenos Aires, 11p

Hormigón. Método de ensayo para determinar la capacidad y la velocidad de succión capilar de agua del hormigón endurecido. IRAM 1871 (2004), Buenos Aires, 12 p.

SIA (2003), Norme Suisse SIA 262/1: "Construction en béton – Spécifications complémentaires", Annexe E: Perméabilité à l'air dans les Structures, pp. 30-31.

G. S. Duffó, S. B. Farina and C. M. Giordano, Characterization of solid embeddable reference electrodes for corrosion monitoring structures. Electrochim. Acta, Vol. 54 (2009), p. 1010-1020.

Reglamento CIRSOC 201-2005 (2005), Reglamento Argentino de Estructuras de Hormigón, INTI, Buenos Aires, 2005, 452 p.

Y.A. Villagrán Zaccardi, C.J. Zega, M.E. Sosa (2012), "¿Cuán apto es el método para medir velocidad de succión capilar cuando es aplicado en hormigones de muy baja capilaridad?", V Congreso Internacional y 19ª Reunión Técnica de la AATH, 7-9 de noviembre de 2012, Bahía Blanca, Argentina, p. 87-94.

Report of the Task Group Reviewing Activities to in the Area of Ageing of Concrete Structures used to Construct Nuclear Power Plant Fuel-Cycle Activities. NEA/CSNI/ R(2002)14. Organization for Economic Co-operation and Development. 101p.

Standard test method for half-cell potential for uncoated reinforcing steel in concrete. ASTM C 876 (1991), Philadelphia.

C. Andrade and C. Alonso, Corrosion rate monitoring in the laboratory and on-site. Construction and Building Materials, Vol. 10 (1996), p. 315-328.